Available online at www.sciencedirect.com

SciVerse ScienceDirect

Journal of the European Ceramic Society 32 (2012) 325–333

www.elsevier.com/locate/jeurceramsoc

Hydrothermal degradation of ground 3Y-TZP

J.A. Muñoz-Tabares [a,*], M. Anglada [a,b]

[a] Departament de Ciència dels Materials i Enginyeria Metallúrgica, Universitat Politècnica de Catalunya, Avda. Diagonal 647 (ETSEIB), 08028 Barcelona, Spain
[b] Centre de Recerca en Nanoenginyeria (CRnE), C. Pascual i Vila 15, 08028 Barcelona, Spain

Received 7 June 2011; received in revised form 11 August 2011; accepted 14 August 2011
Available online 9 September 2011

Abstract

The effect of microstructural changes induced by grinding on the resistance to hydrothermal degradation of 3Y-TZP has been studied. Analyses by X-ray diffraction and μ-Raman spectroscopy have shown that hydrothermal degradation (131 °C/96 h) does not produce additional monoclinic phase in ground specimens. The resistance to degradation of ground samples is explained in terms of the formation of a very thin layer of recrystallised and textured nano-size grains, which prevents the formation of monoclinic variants. In addition, by annealing at 1200 °C during 1 h after grinding, the usual microstructure of as-sintered material is recovered, but the material is still resistance to degradation. This increased resistance for annealed specimens with respect to as sintered specimens is related to the crystallographic texture developed after grinding. The level of texture, as measured by $I_t^{(002)}/I_t^{(200)}$ ratio, diminishes with the annealing treatment and the amount of monoclinic fraction formed during hydrothermal degradation increases proportionally to the reduction in the level of texture.

Keywords: Zirconia; Grinding; Degradation; Microstructure; Texture

1. Introduction

The good combination of strength and toughness of yttria stabilized tetragonal polycrystalline zirconia (3YTZP), as well as its biocompatibility and wear resistance, have allowed its implementation in a wide range of structural applications. Its relatively high fracture toughness is related to the stress-induced transformation of the metastable tetragonal phase to monoclinic phase (referred as t–m transformation).[1] However, this material also suffers a spontaneous t–m phase transformation at the surface when it is exposed to humid environments. This phenomenon, referred to as hydrothermal degradation or low temperature degradation, results in the loss of mechanical properties because of the formation of intergranular microcracks in the surface degraded layer.[2,3]

On the other hand, during final shaping and surface finishing of ceramic devices, different types of machining processes (cutting, grinding, polishing, diamond drilling, sandblasting, CAD/CAM machining, etc.) are required. All these processes induce different types of damage as phase transformation, plastic deformation or cracks that may also affect the structural integrity of these devices.[4,5]

The damage induced by grinding and hydrothermal degradation in service is critical for the manufacture and long term reliability of pieces and components made of 3Y-TZP. In particular, it is important to understand the effect of machining on the resistance to hydrothermal degradation. This point has been studied in 3Y-TZP and it is now well established that grinding increases the resistance to degradation,[6–8] which is usually attributed to the appearance of grinding compressive residual stresses in the surface. However, if the residual stresses are of tensile character, as, for example, in individual wear events at the edge of the track of a scratch, they accelerate the t–m transformation during hydrothermal degradation.[9]

One important observation made long time ago by Whalen et al.[10] is that even if the specimens are annealed after grinding, they do not lose their high resistance to degradation, on the contrary, they become more resistance than specimens in the as-sintered condition. This opens the question of whether the compressive residual stresses are actually essential to explain the degradation resistance of ground specimens. The above authors presented clear evidence that ground samples of 2.45Y-TZP (with 0.6 μm average grain size) become resistant to

* Corresponding author.
E-mail addresses: j.a.munoz.tabares@gmail.com (J.A. Muñoz-Tabares), marc.j.anglada@upc.edu (M. Anglada).

0955-2219/$ – see front matter © 2011 Elsevier Ltd. All rights reserved.
doi:10.1016/j.jeurceramsoc.2011.08.029

hydrothermal degradation by annealing above 1200 °C, after the ground surface has completely recovered its initial tetragonal structure and is free from residual stresses. This was attributed by the authors to the appearance during annealing of recrystallised fine grains at the edge of scratch tracks. Others reports[11,12] have attributed the improvement in the degradation resistance to a decreasing size of the ferroelastic domains, which is supported by experiments on tetragonal-prime zirconia.[12] However the exact mechanism is still not clear.

It is obvious than the exact microstructure induced by grinding on the surface should play an important role on the resistance to hydrothermal degradation. Recently we have studied separately the changes in microstructure that takes place in 3Y-TZP during grinding[13] and hydrothermal degradation[14] by using transmission electron microscopy (TEM) on thin foils extracted from the surface by focus ion beam (FIB). With respect to hydrothermal degradation, it was shown[14] that the monoclinic variants generated at the surface accommodate their transformation shape change by creating a surface relief and they tend to be arranged in parallel bands rather perpendicular to the surface (auto-accommodating variants and autocatalytic propagation [15]). When the variants interact with the grain boundaries, significant tensile stresses are induced which may cause intergranular fracture, leading to the formation of micro-cracks approximately parallel to the surface.[14,16]

With respect to grinding, it was concluded that the main microstructural changes induced by grinding of 3Y-TZP consist of three well defined layers which are described as follows, from the surface to the interior[13]: (1) a crystallized zone, just on the surface, where the grains have a diameter in the range 10–20 nm approximately; (2) a plastically deformed zone; (3) a zone in which tetragonal to monoclinic phase transformation has taken place, which is mainly responsible for the formation of compressive residual stresses that usually increase the flexure strength and apparent fracture toughness of ground specimens.

Our aim in the present paper is to study the resistance to hydrothermal degradation of ground specimens on the basis of the microstructure induced during grinding. To achieve this objective, 3Y-TZP ground samples were hydrothermally degraded by autoclaving in water vapour at 131 °C for periods of time as long as 96 h. The susceptibility to degradation was determined by monitoring the volume fraction of monoclinic phase on the surface in ground and in ground plus annealed specimens, by X-ray diffraction (XRD) and by μ-Raman spectroscopy. The hydrothermal degradation resistance is discussed in the light of the microstructures induced by grinding and by annealing.

2. Experimental procedure

2.1. Material processing

Samples were produced from zirconia powder stabilized with 3% molar of yttria (TZ-3YSB-E, Tosoh, Tokyo, Japan) by cold isostatic pressing and sintering, as described previously.[13,14] The resulting samples denoted "AS" (as sintered) had a grain size of 0.34 ± 0.02 μm and a density of 6.03 ± 0.01 g/cm^3.

2.2. Surface treatments

The samples were ground using a diamond grinding disc (MD-Piano 220 Struers) with a particle size of ∼68 μm, under a pressure of 0.9 MPa with a constant grinding speed of 3.6 m/s and water cooling. This grinding condition was selected from a previous work performed by Juy et al.,[5] who found that the mentioned grinding condition produce the largest increment in mechanical properties and t–m phase transformation. These samples were divided into two sets, the first one corresponds to samples ground as previously described and was denoted as ASgr (AS ground). The second set was denoted as ASgr/ann (AS ground and annealed) and was composed of specimens annealed at 1200 °C after grinding, during different periods of time, with the aim of removing the microstructure changes which occur during grinding and recover the original microstructure of as-sintered specimens.

Finally, the two sets of samples were hydrothermally degraded in an autoclave in the presence of water steam at 131 °C and 0.2 MPa of pressure during 96 h. This long time was chosen with the aim of comparing with AS specimen, which we had studied before under these hydrothermal degradation conditions.[14]

2.3. Surface microstructure

The crystallographic phases were identified by X-ray diffraction (XRD) with Bragg-Brentano symmetric-geometry, using a Philips MRD (Materials Research Diffractometer) system with Cu-Kα (40 kV and 30 mA) radiation. The spectra were obtained in an angle range of $20° \leq 2\theta \leq 87°$, at a scan rate of 10 s/step and with a scan size of 0.017°. Grazing incidence XRD also was conducted, using parallel beam optics with a grazing incident angle (ω) of 1°, which allows a penetration depth of less than 1 μm.

μ-Raman spectroscopy was performed in order to detect and measure the in-depth monoclinic phase distribution after hydrothermal degradation. Raman spectra were collected with a triple monochromator spectrometer T64000 (Horiba/Jobin-Yvon) using an Ar-ion with 514 nm of wavelength as source of excitation. The spectrum integration time was 60 s with averaging the recorded spectra over two successive measurements. The spectra were obtained exploring the sample cross section (polished to mirror surface finish) in steps of ∼1.5 μm. Eq. (1) was used in order to calculate the monoclinic volume fraction (V_m).[17]

$$V_m = \frac{I_m^{181} + I_m^{190}}{0.32(I_t^{147} + I_t^{265}) + I_m^{181} + I_m^{190}} \quad (1)$$

Here, I_m and I_t represent the integrated intensities of monoclinic and tetragonal peaks, respectively, which were calculated using a method described previously,[17] and the numbers identify the Raman shift in cm^{-1}.

The topography of the samples was observed in contact mode in an atomic force microscope (AFM) of digital instruments. The images were treated using WSxM software.[18] To observe

the in depth microstructure by transmission electron microscopy (TEM), a sample was prepared by FIB in a FEI Strata Dual Beam 235 FIB/SEM workstation. TEM observations were performed on a microscope JEOL 1200-EXII operated at 120 keV. In addition, a sample of ASgr/ann was milled by FIB and observed by scanning electron microscopy (SEM).

3. Results

3.1. Hydrothermal degradation of ground specimens

The XRD spectrum obtained from ASgr degraded during 96 h showed the changes previously reported: asymmetric broadening of the (1 1 1) tetragonal peak at ~30° (2θ), inversion of the peaks intensity at 34.64° and 35.22° (2θ) corresponding, respectively, to the planes (0 0 2) and (2 0 0) of the tetragonal phase and, finally, the presence of a small volume fraction of monoclinic phase (~10%), which is equal to that already present in the ground specimens measured with the same technique.[13] It is therefore quite clear that the conditions used here for hydrothermal degradation do not produce any additional increase in monoclinic volume fraction besides that present in the ground material. To confirm this, monoclinic phase profile by μ-Raman spectroscopy was performed on the cross section of an ASgr degraded sample and compared with the profile obtained from an ASgr sample without degradation (Fig. 1b). The use of this technique is convenient in order to determine small concentration of monoclinic phase, due to its high sensitivity compared to XRD (about 0.2% in V_m as determined by the doublet at 181–190 cm^{-1} detectability [19]). Furthermore, the spatial resolution (spot size limit and depth resolution) for μ-Raman spectroscopy can reach a value of 1 μm^3 approximately,[17] related to the quality of the optical equipment (objective) and excitation source used in this work.

The spectra shown in Fig. 1a correspond to the region closer to the surface for both samples. It can be seen that the monoclinic doublet at 180 and 191 cm^{-1} is similar in both spectra. Moreover, the comparison of the transformation profiles shows that the in-depth variation of V_m is also the same in both cases. From these results, it becomes clear that hydrothermal degradation in ground 3Y-TZP does not produce any t–m phase transformation. The small amount of monoclinic phase present was produced during grinding. In principle, it is not surprising that grinding affects strongly the resistant to degradation in view of the severe microstructural changes induced in the surface: phase transformation, plastic deformation, recrystallisation, as well as the presence of significant compressive residual stresses.[13]

3.2. Microstructure of ASgr and its evolution during annealing

Fig. 2 shows 1 μm × 1 μm AFM images from the surface of samples subjected to grinding and annealing. In these images the labels (HE) and (AM) refer to height (topography) and amplitude channels, respectively. In Fig. 2a, the topography of the ASgr sample is characteristic of machined surfaces with

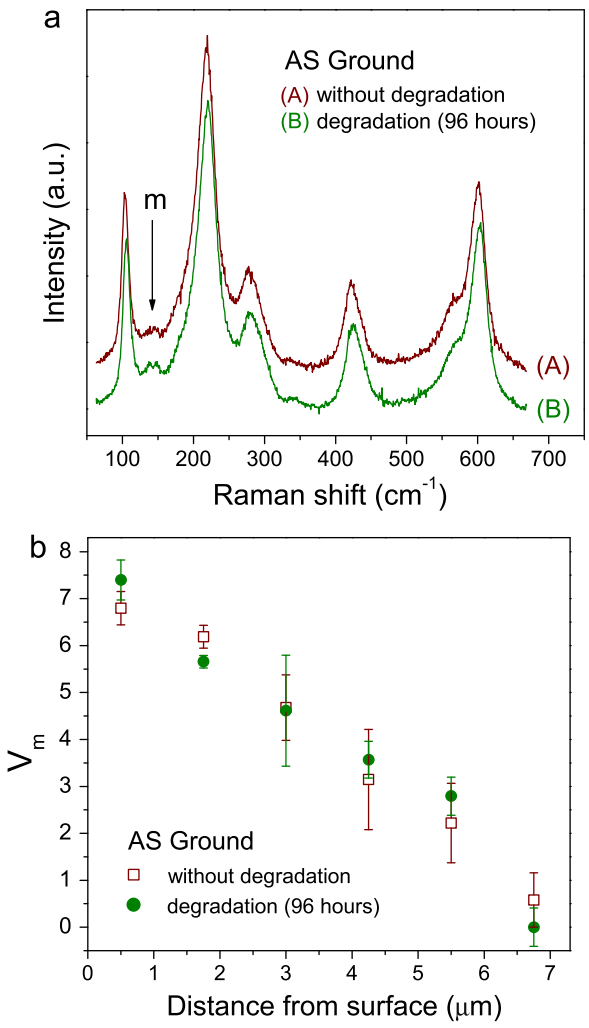

Fig. 1. (a) Raman spectra obtained of the region closer to surface for ASgr, with and without degradation treatment (96 h). It can be seen that the monoclinic doublet at 180 and 191 cm^{-1} is similar in both spectra. (b) Comparison of transformation profiles shows that the in-depth variation of V_m is the same in both cases.

grinding grooves and irregular edges. In this case the specimen was not heat treated to reveal the grain size, since the aim was to show the as ground microstructure avoiding changes that could be induced by heat treatment. This specimen was observed by TEM (Fig. 3) and it was shown that there was a very thin surface layer of recrystallised grains about 10–20 nm in diameter result of in situ recrystallisation. In this mechanism the gradual maladjustment of dislocation cell (in the deformed layer just below, see Fig. 3) respect to initial structure, eventually causes a differences in orientation such that grain sub-boundary are indistinguishable from a large angle grain boundary. This microstructural damage have been recently presented in a detailed study, where each region observed under ground surface (recrystallisation, plastic deformation and phase transformation) was analysed by transmission electron microscopy (TEM) and high resolution (HRTEM).[13]

After 1 min at 1200 °C (with a rate of heating and cooling of 12 °C/min) the grains in ASgr are revealed, showing a microstructure of equiaxed grains (Fig. 2b). The grain size

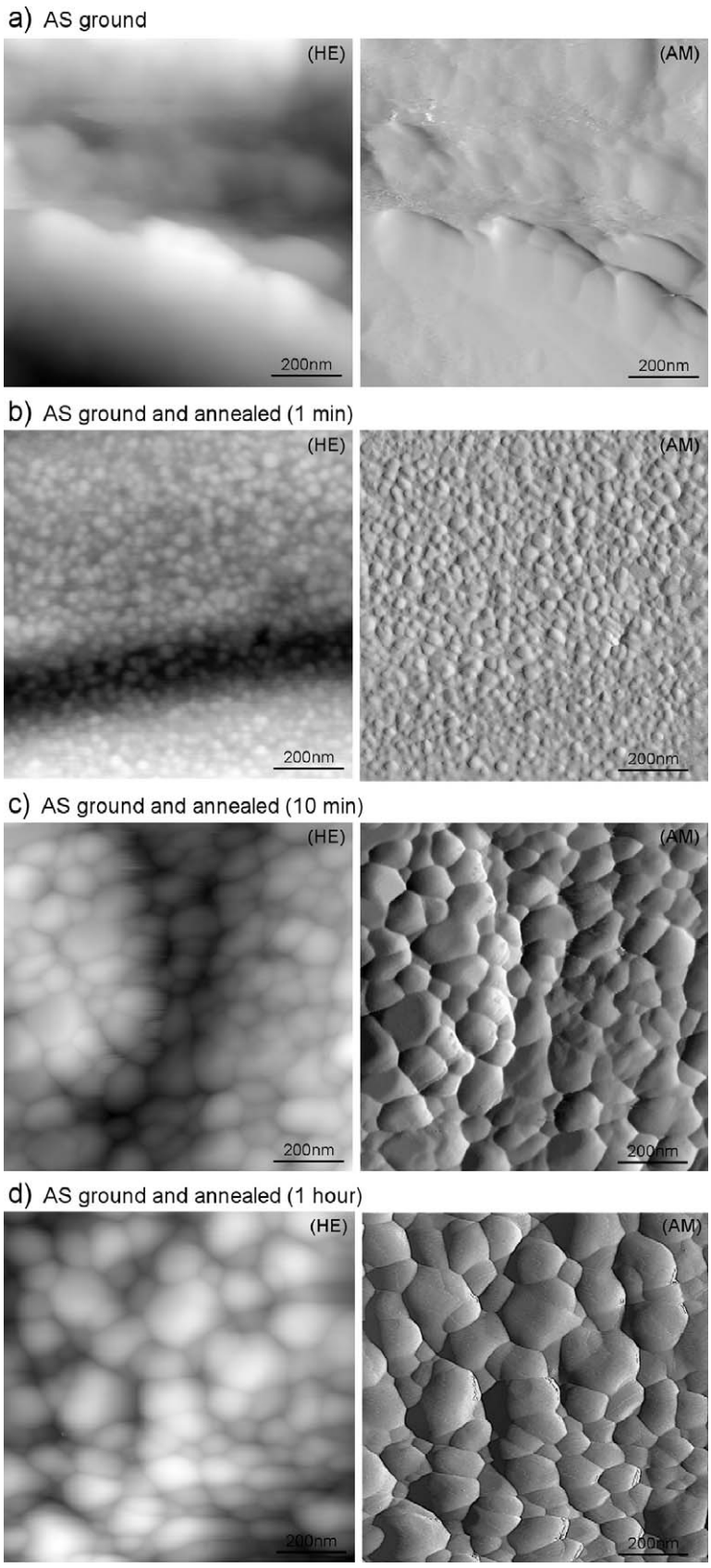

Fig. 2. 1 μm × 1 μm AFM images from the surface of samples subjected to grinding and annealing; the labels (HE) and (AM) refer to height (topography) and amplitude channels, respectively. (a) Ground sample and (b–d) ground and annealed samples at 1200 °C for 1 and 30 min and 1 h, respectively. It can be appreciated that after 1 h the microstructure observed on the surface is similar to the as-sintered material.

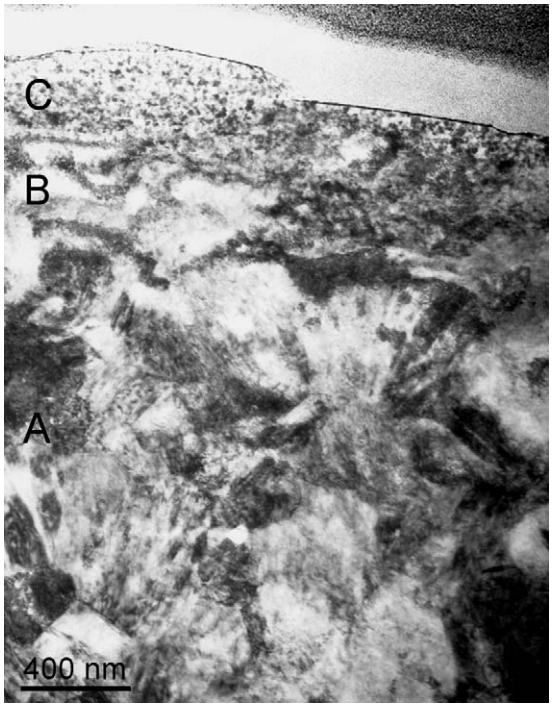

Fig. 3. Subsurface microstructure of ground sample, where three well defined regions are observed: (A) equiaxed grains with martensite plates produced by t–m transformation, (B) microstructure with deformed grains and (C) fine microstructure with grains of ~20 nm diameter.

distribution for this sample (Fig. 4a) shows grains with diameters in a narrow range between 10 and 70 nm and with an average grain size of 30 ± 9 nm. Next, by increasing the annealing time at 1200 °C, the grains grow gradually, reaching an average diameter of 83 ± 33 nm after 10 min (Figs. 2c and 4b). Finally, a size of (284 ± 30 nm) close to the AS material is reached after annealing for 1 h (Fig. 2d and 4c).

On the other hand, a cross-section prepared by FIB in Asgr/ann (1 h) was analysed with the objective to find out the near surface in-depth microstructure. The result is shown in Fig. 5, where it can be appreciated that the different layers observed in the ground sample (Fig. 3) have all disappeared leaving behind a homogeneous microstructure with equiaxed grains of ~300 nm, just below the surface. This result indicates that, for the sample annealed for 1 h, the microstructure observed on the surface (Fig. 2d) is representative of the in-depth microstructure.

3.3. Phase analysis of Asgr/ann (1 h at 1200 °C)

In the XRD spectrum of Asgr/ann annealed for 1 h (Fig. 6), the monoclinic phase produced by grinding has completely disappeared, as evidenced by the absence of the monoclinic peak at 28.2° (2θ) (Fig. 6b). Residual stresses are also removed by annealing, as can be appreciated changes in mechanical properties, as have been demonstrated previously.[13] Thus, the strength, which increased after grinding with respect to as-sintered material from 1197 ± 122 MPa to 1309 ± 110 MPa, recovers in Asgr/ann (1 h) the typical strength of AS.[13] In addition, when a 150 N Vickers indentation is made on this sample, the lengths of indentation cracks, which are shorter (about half) in ASgr with respect to AS,[13] become of similar length as in AS, that is 150 μm approximately (Fig. 7).

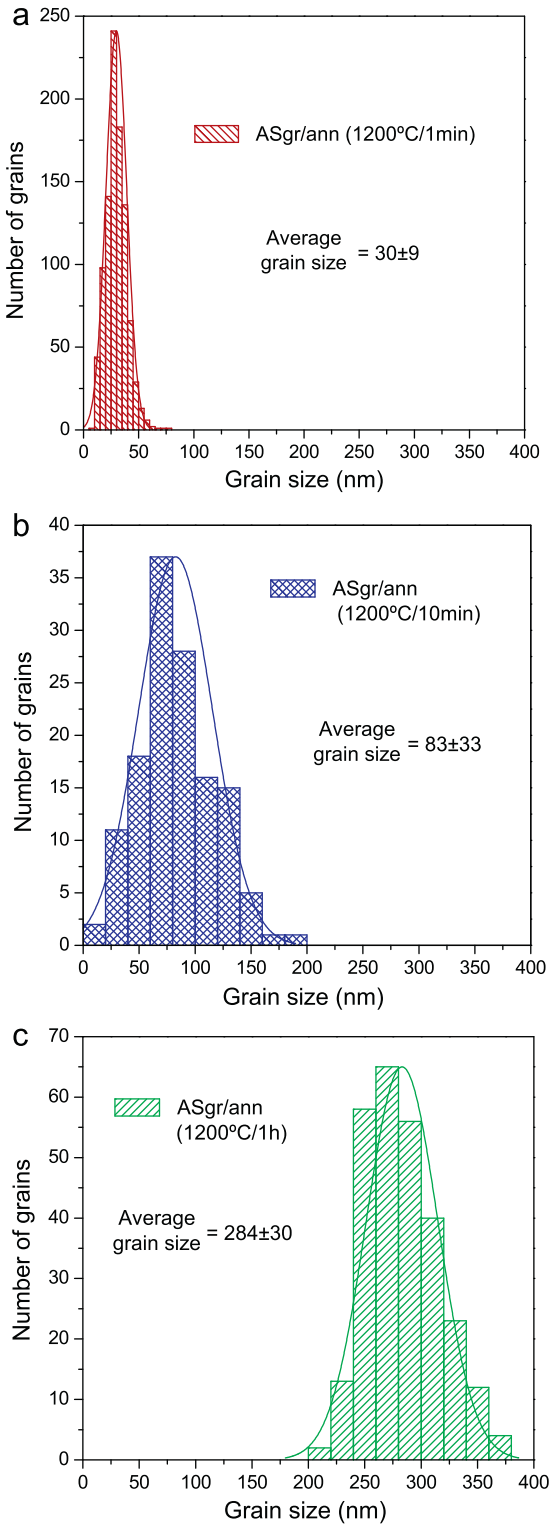

Fig. 4. Grain size distribution for ground and annealed samples at 1200 °C for (a) 1 min, (b) 30 min and (c) 1 h.

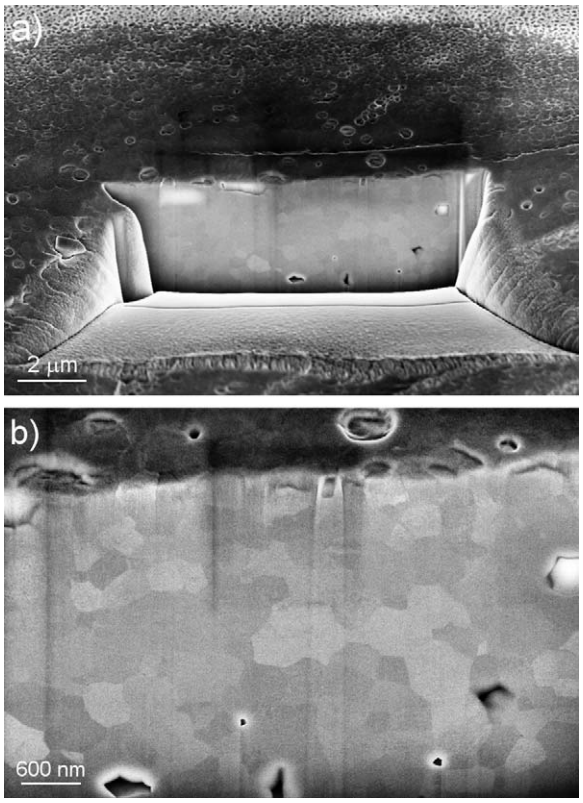

Fig. 5. (a) Cross section of ASgr/ann (1 h) obtained by FIB and (b) microstructure just below the surface; it can be seen that the different layers observed in the ground condition have been eliminated, leaving behind a homogeneous microstructure with equiaxed grains.

The asymmetric broadening of the tetragonal peak at 30° (2θ) also disappears during annealing. However, it is interesting to notice that the inversion of the intensity of the peaks at 34.64° and 35.22° (2θ), which correspond to the planes (0 0 2) and (2 0 0) of the tetragonal phase, persists after annealing. The $I_t^{(0\,0\,2)}/I_t^{(2\,0\,0)}$ intensity ratio for AS is 0.77 and it changes to 1.72 for ASgr. But, in Asgr/ann specimens (1 h annealing) the inversion of the intensity of the peaks remains as can be seen in Fig. 6b. Furthermore, in the spectrum at grazing incidence of the same specimen (Fig. 6c), the intensity of the (0 0 2) tetragonal peak increases with respect to (2 0 0), so that $I_t^{(0\,0\,2)}/I_t^{(2\,0\,0)}$ take a value of ~2.5, that is, higher than in the spectrum of the conventional XRD geometry. This indicates that this crystallographic texture in Asgr/ann is stronger close to the surface, that is, in the region in which strong microstructural changes take place during grinding and annealing.

3.4. Resistance to hydrothermal degradation of Asgr/ann (1 h at 1200 °C)

The degradation test (96 h at 131 °C) was performed in a ground sample after annealing for 1 h, since after this time the microstructure had been largely recovered (Fig. 2d). The XRD spectrum obtained from this sample was similar to that in Fig. 6a, so that no t–m transformation took place during hydrothermal degradation despite the prolonged duration of the hydrothermal treatment (96 h). In addition, measurements were made by μ-Raman spectroscopy in the sample cross section at points near the surface, with the aim to exploit the high resolution of the technique to detect small concentrations of monoclinic phase.[19] The result is presented in Fig. 8, where the monoclinic doublet at 181 and 190 cm^{-1} is not observed, thus confirming the absence of monoclinic phase found by XRD.

Since microstructural changes, as well as the compression residual stresses were removed by annealing for 1 h at 1200 °C, the only difference left was the above mentioned inversion of the intensity, that is, the increase in the intensity of the (0 0 2) tetragonal peak with respect to (2 0 0). Therefore, the different hydrothermal degradation resistance of the ASgr/ann samples could be related to the presence of crystallographic texture in a layer close to the surface.

To gain more insight in the relation between the inversion of the intensity of the peaks and the resistant to degradation, the degree of texture was modified by annealing at 1200 °C for prolonged periods of time (12, 24, 48 and 72 h). After each annealing, the samples were degraded by autoclaving for 96 h and characterized by XRD, measuring each time the volume fraction of monoclinic phase and the $I_t^{(0\,0\,2)}/I_t^{(2\,0\,0)}$ ratio. The result is shown in Fig. 9, where the highest V_m corresponds to AS, which is the one that has the lowest intensity ratio (0.77), while the lowest V_m corresponds to ASgr which has the highest $I_t^{(0\,0\,2)}/I_t^{(2\,0\,0)}$ intensity ratio (1.72). The intermediate points correspond to annealing for 12, 24, 48 and 72 h with corresponding intensity ratios of (1.61), (1.57), (1.51) and (1.44), respectively. From Fig. 9 it is clear that increasing the magnitude of the texture of the tetragonal phase, the appearance of monoclinic phase is delayed making the material more resistant to hydrothermal degradation.

4. Discussion

4.1. Resistance to degradation of specimens ground and annealed for times shorter than 1 h

Hydrothermal degradation is the term used for the phase transformation activated by water species on the surface of tetragonal zirconia in humid environments. When the tetragonal phase is destabilized, the monoclinic variants that form on the surface tend to accommodate the shape change by deforming perpendicularly to the free surface. Thus, when monoclinic plates are formed in a surface grain, it may result in the nucleation of a microcrack at the grain boundary located just below, since the in-depth shape change (accommodated by relief on the surface) will produce local tensile stresses.[14] As the water species diffuse into the material, a second grain, just below the first on the surface, will use the nucleated micro-crack as a free surface to accommodate its own shape change during its transformation. This sequence will be repeated leading to the formation of a transformed micro-cracked layer.[14]

For ASgr, the resistance to hydrothermal degradation is possibly related to the existence of a very thin layer of tetragonal recrystallised nano-grains (10–20 nm) whose size

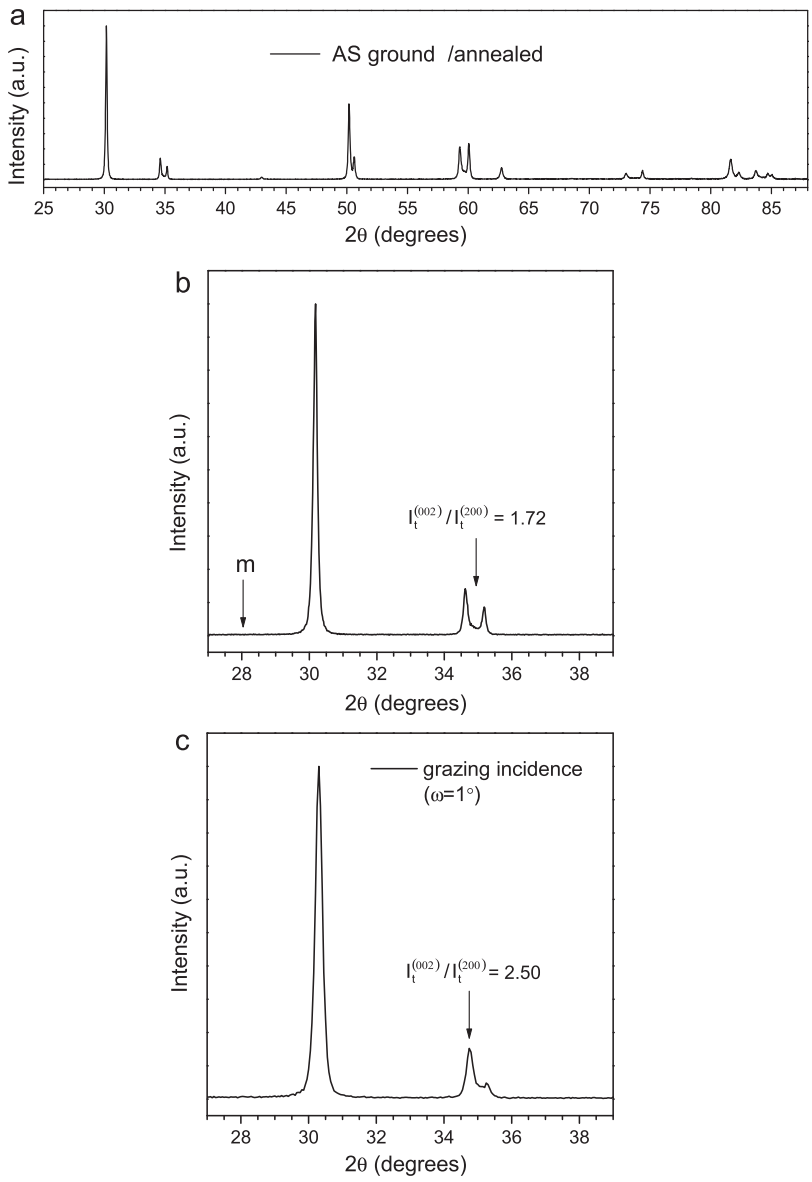

Fig. 6. (a) XRD spectra of AS ground and annealed (1 h) sample, (b) detail of the spectrum shown in the range of 26–37° (2θ), obtained in b) conventional geometry (Bragg–Brentano) and (c) grazing incidence ($\omega = 1°$).

are smaller than the critical size for transformation in humid environment.[20,21] Moreover, when the grain size is in this range (10–20 nm), it has been shown that the tetragonal phase can be stable at room temperature even without the addition of dopants.[22] Another reason for the high degradation resistance of ASgr is the contribution of residual grinding compressive stresses, which will act making more difficult the nucleation of the monoclinic phase because of the expansion associated to the t–m transformation. Although the surface residual compressive stresses are contributing to the higher resistance to degradation, the only presence of recrystallised nano-grains on the surface of ASgr is capable of explaining this effect. Even if water species may diffuse in the nanograin layer, their small size prevents the formation of a martensite nucleous. At higher depth, in the highly deformed layer and in the partly transformed layer by grinding, t–m transformation activated by water species did not take place either, because the sequence transformation/microcracking/transformation that begins at the surface,[14] is inhibited by this layer of nano-grains.

On the other hand, one important effect of annealing on the microstructure of the ground sample is to reverse the ground microstructure to the tetragonal phase free from plastic deformation and residual stresses. In particular, the small amount of monoclinic volume fraction is removed by the m–t phase transformation, which begins at ~600 °C for 3Y-TZP.[23] This reverse transformation, together with the relaxation of compressive residual stress is manifested by the recovery of the apparent fracture toughness (Fig. 7) and mechanical strength.[13] In addition, during annealing there is tetragonal surface grain growth because of the extremely small size of the grain in the recrystallised surface layer after grinding. In the case of ASgr/ann during 1 and 10 min, the grain growth is limited and

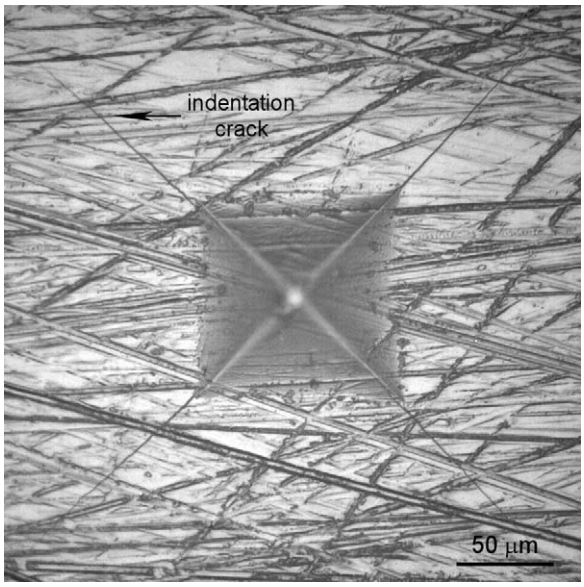

Fig. 7. Vickers indentation at 150 N on Asgr/ann (1 h), where the indentation cracks have a similar length to those observed in AS.

the microstructure obtained has nano-grains whose sizes are still smaller than the critical size for transformation in humid environment. So the resistance to hydrothermal degradation in these samples at the surface can still be explained in terms of the surface layer of tetragonal recrystallised nano-grains.

4.2. Resistance to hydrothermal degradation of Asgr/ann for times equal or longer than 1 h

After 1 h of annealing, the grain size of ASgr/ann is close to that of AS, but its degradation resistance is much larger. It can be noticed that even after 72 h of annealing at 1200 °C, the resistance to degradation of AS/ann is still higher than in AS, in spite of similar grain sizes. If we compare the XRD spectra of ASgr/ann (annealing 1 h or longer) with spectra of AS, we

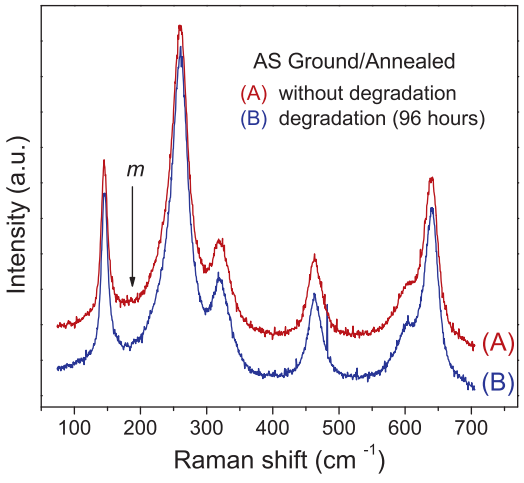

Fig. 8. Raman spectra obtained of the region closer to the surface for ASgr/ann (1 h), with and without degradation treatment (96 h). The monoclinic doublet at 181 and 190 cm^{-1} is not observed, thus confirming the absence of monoclinic phase.

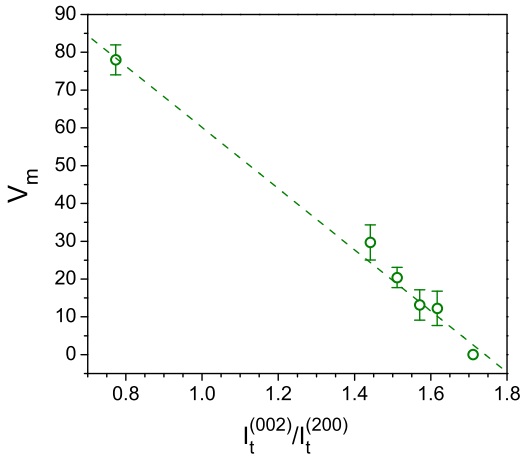

Fig. 9. Monoclinic phase fraction (V_m) produced by hydrothermal degradation (96 h) in terms of the level of texture, as measured by $I_t^{(0\,0\,2)}/I_t^{(2\,0\,0)}$ ratio. The highest V_m corresponds to AS, while the lowest V_m corresponds to ASgr. The intermediate points correspond to samples annealed at 1200 °C for 12, 24, 48 and 72 h.

find that all changes induced by grinding in the spectra have been removed by annealing with the exception of the inversion of the intensities of the (0 0 2) and (2 0 0) peaks. This inversion is already present in ASgr and does not disappear after annealing, which means that a crystallographic texture is developed during grinding. This inversion has been observed by different authors in ground zirconia and different explanations have been proposed.[11,12,24,25] Perhaps the most extended is that based on ferroelastic domains switching during grinding.[12]

From the grazing incidence spectra we have detected that the magnitude of the inversion of the intensity of the (0 0 2) and (2 0 0) tetragonal peaks is larger than under high incidence angles, for which penetration depth is higher, so that this effect is stronger close to the surface. How this texture is induced may be understood by the existence of high residual biaxial compressive stresses at the surface during grinding, which inhibit the t–m transformation. Then, as will be more difficult for the remaining tetragonal phase to transform, it will reorient its c axis (longest) perpendicular to the principal components of the stress (with axes a and b contained in a plane roughly parallel to the surface) in order to accommodate the deformation caused by the biaxial compressive stress, thus reducing the strain energy.[26]

This texture is already present in the nano-grains formed during grinding, as have been observed by HRTEM,[13] and is maintained during annealing. When the material is annealed still deformed grains may recrystallise and the monoclinic phase transforms to tetragonal removing residual stresses. As the same time, recrystallised grains may grow reaching sizes typical of AS after about 1 h at 1200 °C.

Thus, resistance to degradation of ASgr/ann specimens with typical grain size close to 300 nm may only be attributed to the texture of the tetragonal phase (Fig. 6). This is the case of t′-phase zirconia, whose high resistance to hydrothermal degradation has been related to the size of the ferroelastic domains.[11] In the case of the ground 3Y-TZP, it is unlikely that a complete grain of 300 nm in diameter will be reorient and it is more plausible

a partial reorientation.[12] Thereby, inside a single grain (mono-domain) will produce two or more domains that have an effect of domain size reduction. The effect of these domains on hydrothermal degradation resistance has been attributed to the coherence of the domains boundaries, providing a low interfacial energy which hinders the nucleation of the monoclinic phase.[12] An alternative explanation might be related to the lattice correspondence associated to the t–m transformation during degradation. In the case of the transformation of a grain (mono-domain), the martensite plates will contain monoclinic variants rotated 180° relative to each other (equivalent lattice correspondence) mainly of type (100),[27] which occurs in order to accommodate its shear deformation through surface relief. However, the formation of a pair of monoclinic variants in a poly-domain material, where in each domain the tetragonal unit cell is rotated 90° respect to the adjacent domain, implying different lattices correspondences. This mismatch can lead to an increase in the transformation free energy, associated with difference in the lattice strain (Bain strain) between each of the correspondences necessary to complete the transformation.

5. Conclusions

(1) It has been shown that ground 3Y-TZP does not suffer hydrothermal degradation (131 °C/96 h), due to formation by recrystallisation of a very thin surface layer of tetragonal nano-grains from the highly deformed surface, whose size are smaller than the critical size for phase transformation in humid environment.
(2) An annealing treatment at 1200 °C during 1 h after grinding recovers the typical microstructure (phase and grain size) of the as sintered zirconia. However, the texture of the tetragonal phase that appears during grinding is still present after annealing for times larger than 1 h.
(3) The resistance to hydrothermal degradation (131 °C/96 h) of 3Y-TZP ground and annealed (1200 °C/1 hr) is attributed to the presence of texture in the recrystallised surface layer which is gradually weakened during long annealing times. The monoclinic content during degradation was correlated with the level of texture represented by the ratio $I_t^{(002)}/I_t^{(200)}$.

Acknowledgments

This work was supported by Ministerio de Ciencia e Innovación of Spain through Project MAT2008-03398/MAT and by the Generalitat de Catalunya (2009SGR01285). The authors are grateful to E. Jiménez-Piqué, F. Marro and C. Botero from the Centre de Recerca en Nanoenginyeria (CRnE), for their help in the acquisition of AFM and FIB images.

References

1. Garvie RC, Hannink RH, Pascoe RT. *Ceramic steel? Nature* 1975;**258**:703–4.
2. Kobayashi K, Kuwajima H, Masaki T. *Phase change and mechanical properties of ZrO_2–Y_2O_3 solid electrolyte after ageing*. *Solid State Ionics* 1980;**3-4**:489–93.
3. Lawson S. *Environmental degradation of zirconia ceramics*. *J Eur Ceram Soc* 1995;**15**:485–502.
4. Kao H, Ho F, Yang C, Wei W. *Surface machining of fine-grain Y-TZP*. *J Eur Ceram Soc* 2000;**20**:2447–55.
5. Juy A, Anglada M. *Strength and grinding residual stresses of Y-TZP with duplex microstructures*. *Eng Fail Anal* 2009;**16**:2586–97.
6. Sato T, Besshi T, Tada Y. *Effects of surface-finishing condition and annealing on transformation sensitivity of a 3 mol.% Y_2O_3 stabilized tetragonal zirconia surface under interaction of lubricant*. *Wear* 1996;**194**:204–11.
7. Wada S, Yokoyama K. *Difference in the tetragonal to monoclinic phase transformation rate in hot water of 3 mol% Y_2O_3–ZrO_2 ceramics under different surface conditions*. *J Ceram Soc Jpn* 1999;**107**(1):92–5.
8. Kosmac T, Oblak C, Marion L. *The effects of dental grinding and sandblasting on ageing and fatigue behavior of dental zirconia (Y-TZP) ceramics*. *J Eur Ceram Soc* 2008;**28**:1085–90.
9. Deville S, Chevalier J, Gremillard L. *Influence of surface finish and residual stresses on the ageing sensitivity of biomedical grade zirconia*. *Biomaterials* 2006;**27**:2186–92.
10. Whalen PJ, Reidinger F, Antrim RF. *Prevention of low-temperature surface transformation by surface recrystallization in yttria-doped tetragonal zirconia*. *J Am Ceram Soc* 1989;**72**(2):319–21.
11. Jue JF, Chen J, Virkar AV. *Low-temperature aging of t′-zirconia: the role of microstructure on phase stability*. *J Am Ceram Soc* 1991;**74**(8):1811–20.
12. Mehta K, Jue JF, Virkar AV. *Grinding induced texture in ferroelastic tetragonal zirconia*. *J Am Ceram Soc* 1990;**73**(6):1777–9.
13. Muñoz-Tabares JA, Jiménez-Piqué E, Reyes-Gasga J, Anglada M. *Microstructural changes in ground 3Y-TZP and their effect in mechanical properties*. *Acta Mater* 2011;**59**(17):6670–83.
14. Muñoz-Tabares JA, Jiménez-Piqué E, Anglada M. *Subsurface evaluation of hydrothermal degradation of zirconia*. *Acta Mater* 2011;**59**(2):473–84.
15. Kelly P, Rose L. *The martensitic transformation in ceramics: its role in transformation toughening*. *Prog Mater Sci* 2002;**47**:463.
16. Gaillard Y, Jiménez-Piqué E, Soldera F, Mücklich F, Anglada M. *Quantification of hydrothermal degradation in zirconia by nanoindentation*. *Acta Mater* 2008;**56**:4206–16.
17. Muñoz-Tabares JA, Anglada M. *Quantitative analysis of monoclinic phase in 3Y-TZP by Raman spectroscopy*. *J Am Ceram Soc* 2010;**93**(6):1790–5.
18. Horcas I, Fernandez R, Gomez-Rodriguez J, Colchero J, Gomez-Herrero J, Baro A. *WSxM: a software for scanning probe microscopy and a tool for nanotechnology*. *Rev Sci Instrum* 2007;**78**:013705.
19. Kim B-K, Hahn J-W, Han KR. *Quantitative phase analysis in tetragonal-rich tetragonal/monoclinic two phase zirconia by Raman spectroscopy*. *J Mater Sci Lett* 1997;**16**(8):669–71.
20. Evans AG, Burlingame N, Drory M, Kriven WM. *Martensitic transformations in zirconia particle size effects and toughening*. *Acta Metall* 1981;**29**:447–56.
21. Lange FF. *Transformation toughening. Part 1: Size effects associated with the thermodynamics of constrained transformations*. *J Mater Sci* 1982;**17**:225–34.
22. Shukla S, Seal S. *Mechanisms of room temperature metastable tetragonal phase stabilisation in zirconia*. *Int Mater Rev* 2005;**50**:45–64.
23. Fabrichnaya O, Aldinger F. *Assessment of thermodynamic parameters in the system ZrO_2–Y_2O_3–Al_2O_3*. *Int J Mater Res* 2004;**95**:27–39.
24. Swain MV, Hannink RHJ. *Metastability of the martensitic transformation in a 12 mol% ceria–zirconia alloy: II. Grinding studies*. *J Am Ceram Soc* 1989;**72**:1358–64.
25. Zhu H-Y. *Grinding induced t–m martensitic transformations and texture in a 12 mol% ceria doped tetragonal and monoclinic zirconia*. *J Mater Sci Lett* 1996;**15**:606–9.
26. Chien FR, Bic FJ, Prakash V, Heuer AH. *Stress-induced martensitic transformation and ferroelastic deformation adjacent microhardness indents in tetragonal zirconia single crystals*. *Acta Mater* 1998;**46**(6):2151–71.
27. Hayakawa H, Adachi K, Oka M. *Crystallography analysis of the monoclinic herringbone structure in arc-melted ZrO_2 2 mol% Y_2O_3 alloy*. *Acta Metall Mater* 1990;**38**(9):1753–9.